APPENDIX A

Drill core logs

Table A.1 List of drill core logs provided digitally on accompanying DVD

Dril hole	Location	Chapter	Metres logged		
			From	To	Total
DDHL712	Lienetz	Ch. 5	115.0	273.9	158.9 m
DDHL757	Lienetz	Ch. 5	67.0	364.2	297.2 m
DDHL791	Lienetz	Ch. 5	67.3	340.0	272.7 m
DDHL1160	Lienetz	Ch. 5	142.9	321.6	178.7 m
DDHL1285	Lienetz	Ch. 5	32.5	59.0	16.5 m
DDHL1408	Minifie	Ch. 4	4.0	105.1	101.1 m
DDHL1415	Minifie	Ch. 4	7.57	170.0	162.43 m
DDHL1446	Minifie	Ch. 4	0	170.9	170.9 m
DDHL1448	Minifie	Ch. 4	0	155.4	155.4 m
DDHL1449	Minifie	Ch. 4	0	140.7	140.7 m
DDHL1450	Minifie	Ch. 4	7	115.0	108.0 m
DDHL1455	Minifie	Ch. 4	0	150.0	150.0 m
DDHL1456	Minifie	Ch. 4	0	155.0	155.0 m
DDHL1703	Lienetz	Ch. 5	6.5	150.0	143.5 m
DDHL1704	Lienetz	Ch. 5	6.8	150.0	143.2 m
DDHL1708	Lienetz	Ch. 5	9.7	143.2	90.3 m
GW29	Luise volcano	Ch. 3	10.0	777.7	167.7 m
GW30	Luise volcano	Ch. 3	329.9	859.3	529.7 m
GW31	Luise volcano	Ch. 3	67.6	768.0	700.4 m
GW32	Luise volcano	Ch. 3	67.0	922.0	855.0 m
GW33	Luise volcano	Ch. 3	4.8	811.0	806.2 m
GW34	Luise volcano	Ch. 3	22.0	786.0	764.0 m

APPENDIX B

Open pit maps

Table B.1 List of open pit mapping data provided digitally on accompanying D

Pit map	Benches
2006 Minifie pit mapping data	872
	884
	956
	980
2007 Lienetz pit mapping data	854
	925
	Ramp
	968
	980
2008 Lienetz pit mapping data 1 of 2	884
	920
2008 Lienetz pit mapping data 2 of 2	Phase 6 ramp
	920
	944
	992

APPENDIX C

XRF geochemistry

C.1 Sampling and analytical techniques

Major and trace element compositions of seven coherent lavas and intrusions (Table C.1) from the Luise volcanic block were analysed by X-ray fluorescence (XRF) at the University of Tasmania. Two samples are from the Minifie ore zone, four from the Lienetz ore zone and one from Apudontes Quarry on the northern flank of the Luise volcano. The aim of this study is to assign geochemical nomenclature to supplement each of the coherent facies descriptions and does not aim to be a detailed lithogeochemical study. Analyses have been interpreted with caution due to the absence of less altered examples, the proximity to the Ladolam ore deposit and the presence of hydrothermal alteration minerals observed in thin section and hand sample.

Rocks were first crushed in a hydraulic crusher. Fragments were hand-picked to exclude chips with oxidised or weathered rinds, veins or amygdales and were powdered in a tungsten carbide disc mill. Major element and trace element concentrations were determined on a Philips automated XRF spectrometer at the University of Tasmania using standard fused disc and pressed pellet techniques (Watson, 1996; Robinson, 2003). The major element analyses have been recalculated to 100 % anhydrous to remove variations caused by differing loss on ignition values.

C.2 Element mobility

In the study area, hydrothermal alteration is locally intense. Therefore all samples selected for this study have undergone some degree of mineralogical readjustment. The variable mobility of elements during hydrothermal alteration is relatively well documented (e.g. Rollinson, 1993; Gifkins et al., 2005). Elements considered to be essentially immobile during this style of alteration include high field strength elements such as Ti, Zr, Nb and Y.

In these analyses there is discrepancy between discrimination diagrams based on SiO_2, K_2O and Na_2O (Figs. C.1a and C.1c) and diagrams based on immobile elements (Figs. C.1b and C.2d) and major elements are interpreted to have undergone mineralogical readjustment.

Table C.1 XRF major and trace element analyses of coherent facies of the Luise volcanic block

	Sample	8020	8021	8022	8023	8024	8025	DDHL1415 166.12
	Locality	Lienetz 980 Bench	Minifie 972 Bench	Lienetz 920 Bench	Lienetz Ph. 6 ramp	Lienetz Ph. 6 ramp	Apudontes Quarry	Minifie DDHL1415
	Lithology	Andesite	Andesite	Basalt	Microdiorite	Syenite	Basalt	Basalt
Major elements (wt %)	SiO_2	57.59	52.34	45.48	49.32	55.59	48.62	49.06
	TiO_2	0.52	0.84	0.98	0.91	0.47	0.92	0.88
	Al_2O_3	20.06	18.64	19.78	18.01	18.40	13.86	13.51
	[1] Fe_2O_3	4.23	9.22	11.25	10.01	4.16	11.63	11.41
	MnO	0.17	0.35	0.26	0.26	0.13	0.25	0.29
	MgO	1.60	2.32	2.95	4.28	1.58	6.29	7.40
	CaO	6.47	10.26	12.31	9.27	5.19	13.46	11.37
	Na_2O	5.23	2.84	2.73	2.59	0.48	3.57	3.00
	K_2O	3.83	2.77	3.50	4.78	13.74	0.91	2.76
	P_2O_5	0.30	0.41	0.77	0.57	0.27	0.50	0.32
	S	0.17	1.75	0.04	0.19	3.51	<0.01	0.23
	[2] Total	100	100	100	100	100	100	100
	L.O.I	5.65	8.65	10.90	2.01	6.47	2.83	1.97
Trace elements (ppm)	As	<4	7	<4	18	426	<4	35
	Ba	337	324	462	271	694	210	228
	Bi	<2	<2	<2	<2	<2	<2	<2
	Ce	32	27	43	27	34	33	21
	Cr	2	9	6	6	1	166	156
	Cu	92	89	278	215	32	154	131
	La	15	9	18	11	3	15	10
	Nb	3	1	3	<1	2	<1	1
	Nd	19	16	28	18	9	20	17
	Ni	3	6	10	10	2	39	44
	Pb	15	6	10	12	39	5	7
	Rb	73	31	38	76	184	79	67
	Sc	6	17	15	18	6	36	24
	Sn	<2	<2	2	<2	<2	<2	not determ.
	Sr	1795	1107	2670	1394	1454	1202	861
	Ti	3117	5036	5875	5455	2818	5515	5276
	Th	3	<1.5	<1.5	<1.5	<1.5	2	<1.5
	U	2	<1.5	<1.5	<1.5	<1.5	<1.5	<1.5
	V	176	283	398	292	207	348	326
	Y	18	20	22	21	9	19	19
	Zn	68	75	80	105	65	87	92
	Zr	95	74	77	71	77	58	55
	Zr / Ti	0.03	0.01	0.01	0.01	0.03	0.01	0.01
	Nb / Y	0.16	0.07	0.13	0.05	0.26	0.05	0.08
	Zr / TiO_2	184.40	87.13	78.17	77.38	164.92	63.23	62.02

[1] Total Fe as Fe_2O_3

[2] Analyses recalculated to 100% anhydrous

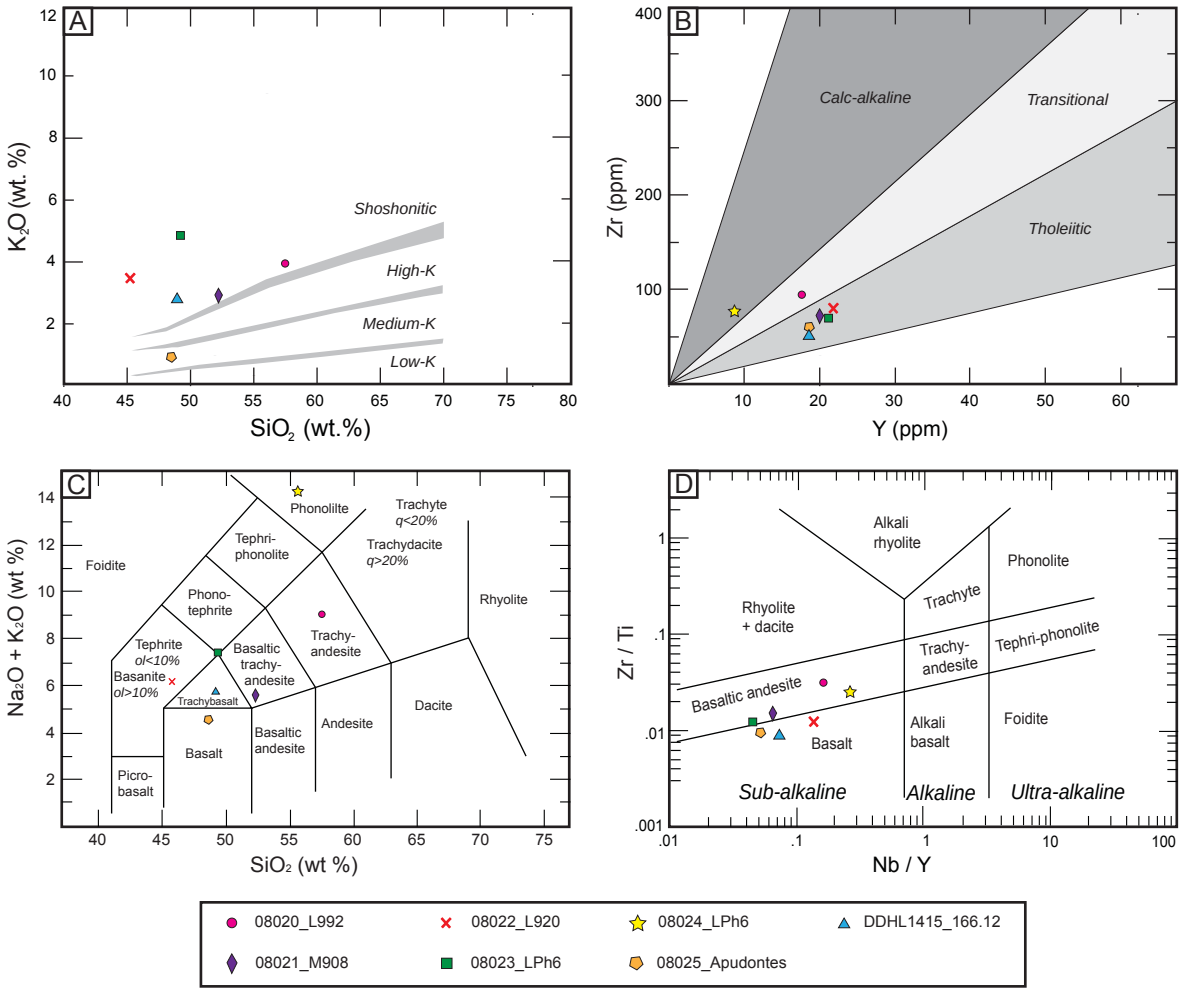

Figure C.1 Major and trace element discrimination diagrams for volcanic and subvolcanic rocks of the Luise volcanic edifice. (A) K_2O vs SiO_2 diagram with magma series boundaries after Percerillo and Taylor (1976). (B) Y-Zr incompatible element plot used for determination of magmatic affinities in altered volcanic rocks (from MacLean and Barrett, 1993). (C) Total alkali-silica (TAS) diagram of Le Maitre (1989), showing rock fields defined on the basis of $Na_2O + K_2O$ vs SiO_2. (D) Zr/Ti vs Nb/Y trace element discrimination plot from Pearce (1996).

The Zr/Ti versus Nb/Y discrimination diagram (Fig. 2.1d) from Pearce (1996) is interpreted to reflect more accurate rock names than the discrimination diagram of Le Maitre (1989) because of the effects of K-metosomatism on the samples. The Zr versus Y plot of MacLean and Barrett (1993) show the cluster of rocks types in when plotted using immobile elements versus that of SiO_2 versus K_2O. The scatter of rock types in Figure C.1a is interpreted to be the result of K-metosomatism of these mobile elements.

C.3 Compositions

Previous studies (Johnson et al., 1976; Heming, 1979; Wallace et al., 1983; Kennedy et al., 1990a; Kennedy et al., 1990b; McInnes and Cameron, 1994; Stracke and Hegner, 1998;

Muller et al., 2001; Muller et al., 2003) demonstrated a predominance of rocks with high-K calc-alkaline to shoshonitic compositions on Lihir Island and throughout the TLTF island chain. In a plot of the SiO_2 versus K_2O (Fig C.1a) plot of Percerillo and Taylor (1976), the new data conform to the regional pattern. The compositions of coherent rocks are similar throughout the Luise volcanic block and plot within the basalt to andesite fields (Figs. C.1d). Samples 08023 and 08024 are named with plutonic rock names (microdiorite and syenite respectively) based on their modal mineralogy. Plutonic names were chosen to highlight that they are equigranular or have an equigranular groundmass and are coarser grained that the other rock types analysed.

APPENDIX D

U-series geochronology

D.1 U-series geochronology

This appendix supplements section 3.4 (Quaternary limestone) where the motivation behind applying the dating technique, limestone sample selection, U-series dating systematics, analytical methods and results are discussed.

D.2 U-Series dating systematics

Short-lived daughter isotopes in the α-decay chains of long-lived ^{238}U (Fig. D.1), ^{235}U and ^{232}Th provide a number of useful dating tools for young (late Quaternary) systems (Dickin, 1995). Fossil corals can be dated using several of these tools, notably ^{234}U-^{238}U and ^{234}U-^{230}Th (Chen et al., 1986; Edwards et al., 1987). A distinctive property of the U-series nuclides which sets them apart from the other dating schemes is that the radiogenic daughters are also radioactive (Dickin, 1995). Secular disequilibrium is achieved when different nuclides in the decay series become fractionated during geologic processes such as erosion, sedimentation,

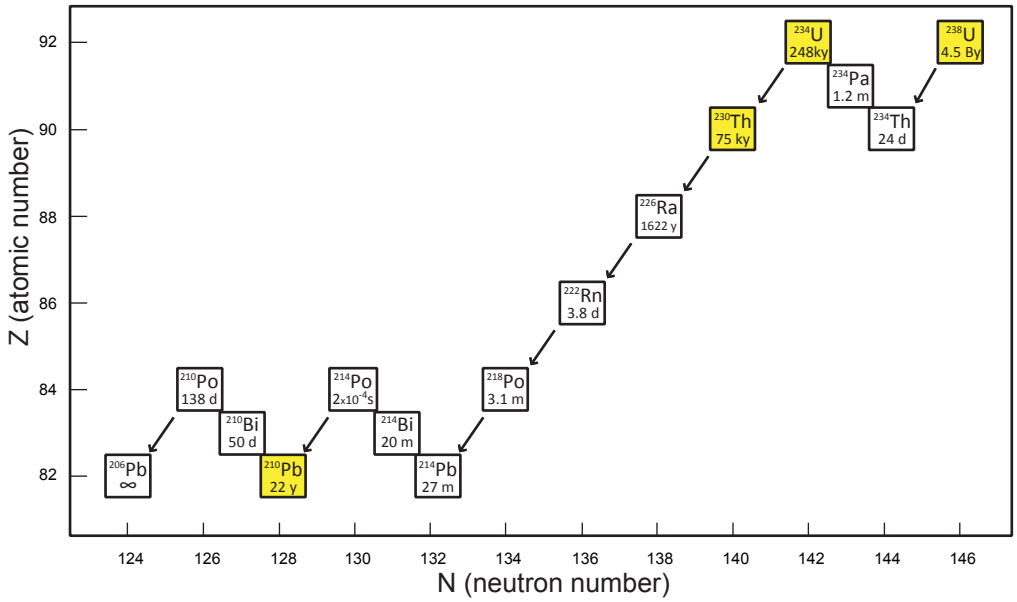

Figure 3.14 Species in the Th- and U-series decay chains and their half lives (from Dickin, 1995). Species used in this study are indicated by yellow boxes. Half lives are reported in s (seconds), m (minutes), d (days), y (years), ky (thousand years), By (billion years).

melting or crystallisation (Dickin, 1995). As a chronological tool, the secular disequilibrium is used in two ways, as the daughter-excess and daughter-deficiency dating methods (Dickin, 1995).

^{234}U – ^{238}U daughter-excess method (<1.5 Ma)

The ^{234}U - ^{238}U method relies on the decay of excess ^{234}U in seawater-derived solids (such as corals). Excess ^{234}U in seawater is the result of preferential mobilisation of ^{234}U during weathering (Dickin, 1995). Because U has a relatively long residence time in seawater (>300 kyr; Ku et al., 1977), it is thought to have a constant $^{234}U/^{238}U$ ratio in the geologic past. The ^{234}U activity ratio ($(^{234}U/^{238}U)_A$) is 1.143 (Chen et al., 1986). Live corals incorporate ~3 to 4 ppm U from seawater and inherit its $^{234}U/^{238}U$. When U uptake ceases (i.e. the coral dies) the excess ^{234}U decays away until secular equilibrium ($(^{234}U/^{238}U)_A=1$) is restored. This process takes ~1.5 million years (Dickin, 1995). The ^{234}U age is determined from the ^{234}U excess remaining today. The method can only be applied where the initial ^{234}U excess is known, such as undisturbed marine deposits of Quaternary age. Uplifted limestone is difficult to date because coral which has been exposed to fresh water is very susceptible to open-system behaviour (Dickin, 1995).

^{230}Th – ^{234}U daughter-deficiency method (<500,000 years)

The ^{230}Th-^{234}U method, also known as U-Th, is used for samples characterised by high to very high initial $^{238}U/^{232}Th$ and $^{238}U/^{230}Th$, such as freshwater and marine calcite / aragonite which tend to exclude Th. Over time, the initial deficiency of ^{230}Th, the daughter of ^{234}U, is erased as $^{234}U/^{230}Th$ is driven back to secular equilibrium. A U-Th age can be determined by measuring $^{234}U/^{230}Th$ and $^{234}U/^{238}U$. The half lives (Fig. D.1) of the two nuclides involved, ^{234}U (248 kyr) and 230^{Th} (75 kyr), constrain the useful range of the technique to the last 400 to 500 kyr (Dickin, 1995). The U-Th method is applicable to the dating of any closed-system carbonate which is free from contamination by initial detrital thorium.

D.3 Samples and analytical methods

The U-series methods have been applied to young marine and fresh-water carbonates with great success (e.g. Bard et al., 1996; Esat et al., 1999; Drysdale et al., 2009). However, while analytically straightforward using modern mass spectrometric methods, application of U-Th and ^{234}U dating to corals can be fraught with potential problems (Edwards et al., 2003). Dead coral is very sensitive to post-depositional geochemical changes, notably redistribution of U, both under water and when exposed to subaerial weathering. U mobility tends to produce spurious U-Th ages that are older than the real ages. Criteria used to reject altered corals from analysis, or to reject coral ages, include: (i) $^{234}U/^{238}U_{initial}$ must be in the range of $^{234}U/^{238}U_{seawater}$, between 1.152 and 1, (ii) total ^{238}U must be in the range of modern analogues, and depending on the coral species, values should be between 2.1 and 3.84 ppm, (iii) the absence of detrital Th contamination should be confidently established (^{232}Th levels should be below 2 ppb) and (iv) the recrystallised calcite content must be lower than 2% (Scholz and Mangini, 2007).

The nine limestone samples were examined in terms of textural and compositional heterogeneity in order to assess the degree of alteration and satisfy the above criteria. The samples were imaged using X-radiograph negative prints (Fig. D.2b) by Paul Edwards of X-Ray Hobart to visually estimate areas of diagenetic alteration after the method of Scholz et al. (2004). Petrographic examination indicates that all samples (except Lmst1) had undergone some degree of calcite recrystallisation. Using density gradients (Fig. D.2c) from the X-radiograph negatives and textural zones identified under reflected light petrography, the locations of trace element spot analyses were selected.

After initial petrographic screening, the nine samples were prepared in mounts for LA-ICPMS (laser-ablation inductively coupled-mass-spectrometer) trace element spot analysis at the University of Tasmania to determine whether samples had appropriate levels of U, Th and Pb and to determine which samples were likely to have detrital Th contamination. Each analysis on the Agilent 7500cs ICPMS coupled to the New Wave UP193 solid state laser ablation microprobe was set to 10 Hz frequency and 100% energy burned a 100 μm diameter spot size (the complete data set is provided in Table D.1). An example of data used in the

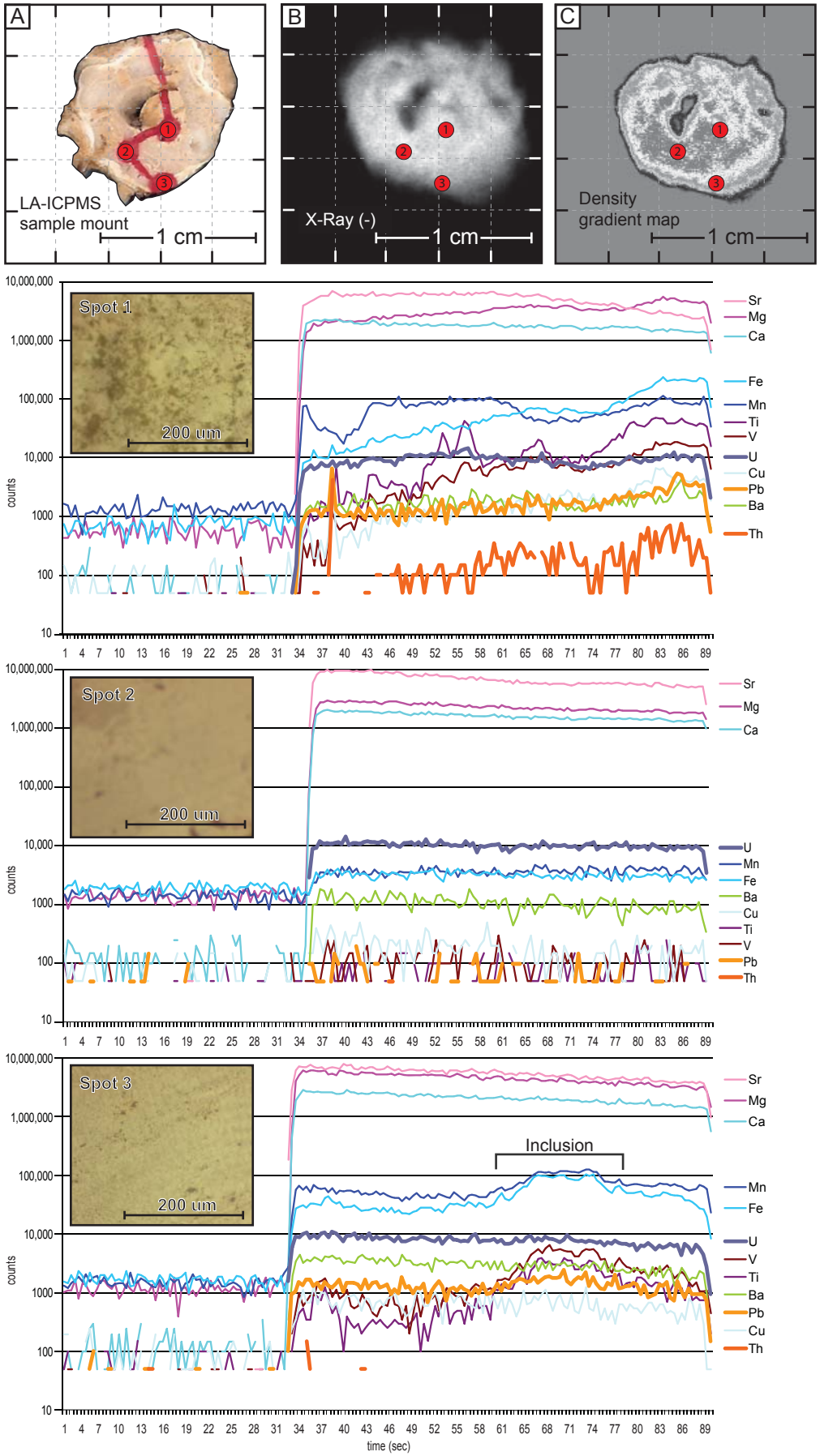

Figure 3.15 LA-ICPMS analyses of three spots in limestone sample 6. Corresponding textures shown as insets on the graphs. The location of spot analyses are shown in (A) the sample mount, (B) the corresponding X-radiograph negative image and (C) the density gradient map. Spot 1 is heterogeneous and has a number of inclusions, spot 2 is pure carbonate and spot 3 has a Mn, Fe, V, Ba rich inclusion.

sample selection process is provided in Figure D.2.

In the preliminary analyses of the nine samples, three (Lmst 1, 6 and 7) had the required U, Th and Pb levels, were free of inclusions and were homogenous or had homogenous zones that were easily extractable. Of these three samples, two (Lmst 6 and 7) had more than 2% calcite and are suspected to have undergone diagenetic alteration. Although alteration is a problem in Lmst 6 and 7, they were submitted for U-Th dating along with unaltered Lmst 1, in the hope of extracting maximum ages. Two sub-samples were analysed from Lmst 6 to assess within-sample age variability.

Table D.1 List of LA-ICPMS analysis files provided digitally on accompanying DVD

Filename	Sample name	Spot analysis		Mineral	Energy (J/cm^2)	Spot size
		Area	Burn			
JA16B01	NIST612	-	-	glass (primary standard)	2.8	100 um
JA16B02	NIST612	-	-	glass (primary standard)	2.7	100 um
JA16B03	Lmst1	1	1	carbonate	2.8	100 um
JA16B04			2	carbonate	2.7	100 um
JA16B05		2	1	carbonate	2.7	100 um
JA16B06			2	carbonate	2.7	100 um
JA16B07		3	1	carbonate	2.8	100 um
JA16B08			2	carbonate	2.65	100 um
JA16B09	Lmst2	3	1	carbonate	2.6	100 um
JA16B10			2	carbonate	2.6	100 um
JA16B11		2	1	carbonate	2.6	100 um
JA16B12		1	1	carbonate	2.6	100 um
JA16B13			2	carbonate	2.7	100 um
JA16B14	Lmst3	1	1	carbonate	2.6	100 um
JA16B15		2	1	carbonate	2.53	100 um
JA16B16			2	carbonate	2.6	100 um
JA16B17			3	carbonate	2.6	100 um
JA16B18		3	1	carbonate	2.6	100 um
JA16B19			2	carbonate	2.6	100 um
JA16B20		4	1	carbonate	2.6	100 um
JA16B21			2	carbonate	2.7	100 um
JA16B22	NIST612	-	-	glass (primary standard)	2.75	100 um
JA16B23	NIST612	-	-	glass (primary standard)	2.56	100 um
JA16B24	NIST612	-	-	glass (primary standard)	2.73	100 um
JA16B25	NIST613	-	-	glass	2.54	100 um
JA16B26	Lmst5	1	1	carbonate	2.74	100 um
JA16B27			2	carbonate	2.76	100 um
JA16B28		2	1	carbonate	2.69	100 um
JA16B29			2	carbonate	2.63	100 um
JA16B30		3	1	carbonate	2.68	100 um
JA16B31			2	carbonate	2.63	100 um

Filename	Sample name	Spot analysis		Mineral	Energy (J/cm²)	Spot size
		Area	Burn			
JA16B32	Lmst6	1	1	carbonate	2.77	100 um
JA16B33			2	carbonate	2.65	100 um
JA16B34		2	1	carbonate	2.66	100 um
JA16B35			2	carbonate	2.71	100 um
JA16B36		3	1	carbonate	2.64	100 um
JA16B37			2	carbonate	2.56	100 um
JA16B38	Lmst7	1	1	carbonate	2.63	100 um
JA16B39			2	carbonate	2.52	100 um
JA16B40			3	carbonate	2.65	100 um
JA16B41		2	1	carbonate	2.61	100 um
JA16B42			2	carbonate	2.63	100 um
JA16B43		3	1	carbonate	2.62	100 um
JA16B44			2	carbonate	2.59	100 um
JA16B45		4	1	carbonate	2.57	100 um
JA16B46			2	carbonate	2.57	100 um
JA16B47	NIST612	-	-	glass (primary standard)	2.51	100 um
JA16B48	NIST612	-	-	glass (primary standard)	2.55	100 um
JA16B49	NIST612	-	-	glass (primary standard)	2.65	100 um
JA16B50	NIST612	-	-	glass (primary standard)	2.58	100 um
JA16B51	Lmst9.3	1	1	carbonate	2.65	100 um
JA16B52			2	carbonate	2.75	100 um
JA16B53		2	1	carbonate	2.61	100 um
JA16B54		3	1	carbonate	2.62	100 um
JA16B55			2	carbonate	2.6	100 um
JA16B56		4	1	carbonate	2.73	100 um
JA16B57			2	carbonate	2.58	100 um
JA16B58	Macs-3	-	-	press (secondary standard)	2.68	100 um
JA16B59	Macs-3	-	-	press (secondary standard)	2.5	100 um
JA16B60	NIST612	-	-	glass (primary standard)	2.63	100 um
JA16B61	NIST612	-	-	glass (primary standard)	2.48	100 um

Table notes: For each spot analysis the frequency was set at 10 Hz and the energy was 100%.

Because the age of the Lihir limestone is known to be early Pliocene or younger, we planned to apply three methods in order of age resolution and analytical precision. The first was $^{230}Th - ^{234}U$ which has a resolution <500,000 years. The second was $^{234}U - ^{238}U$ and has a resolution <1.5 million years. If the limestone proved to be older than 1.5 Ma, U-Pb would be applied. To accommodate the potential of using all three techniques, 250 mg of each sample was required: 20 mg for U-Th, 30 mg for ^{234}U and 100 to 200 mg for U-Pb.

The U-series isotope analyses (Table D.2) were done at the University of Melbourne, following the technique described in Hellstrom (2003). Small chips of coralline limestone (<10 mg) were slowly dissolved in weak nitric acid and spiked with mixed ^{233}U-^{239}Th tracer,

followed by extraction of Th and U in a single fraction on EICHROM TRU resin (Luo et al., 1997). Activity ratios $^{230}Th/^{234}U$ and $^{234}U/^{238}U$ were measured simultaneously by multi-collector ICPMS.

Table D.2 ^{230}Th-^{234}U results
(analysed by J. Hellstrom at the University of Melbourne - September 2009)

Sample name	238/V	230/238 activity	95% ext.	234/238 activity	95% ext.	Age (Ka)	95%err	232/238 activity	2SE	230/232i	2sd
Lmst1	3.33	0.002	0.000	1.150	0.002	0.179	0.024	0.000	0.000	1.00	0.50
Lmst6	1.97	0.989	0.003	1.093	0.002	234.821	2.977	0.002	0.000	1.00	0.50
Lmst7	2.89	0.935	0.004	1.107	0.002	190.629	2.170	0.000	0.000	1.00	0.50
Lmst6x	1.48	1.023	0.004	1.087	0.003	273.881	5.074	0.001	0.000	1.00	0.50

Sample name	234/238Ai	95%err	230/232 activity	Corrected age (Ka)	2se	Corrected 230/232 activity	2se	Corrected Age/Age
Lmst1	1.151	0.002	71.6	0.177	0.028	1.151	0.003	99%
Lmst6	1.182	0.004	609.2	234.679	3.331	1.182	0.004	100%
Lmst7	1.184	0.004	6071.2	190.628	2.396	1.184	0.003	100%
Lmst6x	1.189	0.005	1772.4	273.963	5.770	1.189	0.004	100%

APPENDIX E

Ar-Ar geochronology

E.1 Sampling

^{40}Ar / ^{39}Ar geochronology was used to constrain the age and/or cooling history of rock units in the area of the Ladolam gold deposit. Only one unit in the study area contained the appropriate mineralogy for the study – a plagioclase-phyric andesite (L8) that is interpreted to be a shallow level dykes that are spatially and temporally related to the polymictic, accretionary lapilli-bearing, matrix-supported breccia (L7). L8 and L7 are the youngest units at Lienetz, interpreted to be younger than the ore-forming event and the steam-heated blanket.

Amphibole selected for ^{40}Ar / ^{39}Ar geochronology contains glassy melt inclusions and does not contain secondary biotite, chalcopyrite, or other alteration minerals that may reset the isochrons. The sample location and isotopic data are shown in Table E.1 and results are shown in Figure E.1.

E.2 Methodology

Each sample was crushed and sieved to obtain fragments ranging in the size range from 0.3 to 2 mm. A hand magnet was passed over the samples to remove magnetic minerals and metallic crusher fragments / spall. The samples were washed in deionised water, rinsed and then air-dried at room temperature.

Mineral separates were hand-picked, wrapped in aluminium foil and stacked in an irradiation capsule with similar-aged samples and neutron flux monitors (Fish Canyon Tuff sanidine; 28.02 Ma (Renne et al., 1998)). The samples were irradiated at the McMaster Nuclear Reactor in Hamilton, Ontario, for 56 MWH, with a neutron flux of approximately 3 x 10^{16} neutrons / cm^2. Analyses (n=54) or 18 neutron flux monitor positions produced errors of < 0.5 % in the calculated J value.

Table E.1 Ar-Ar isotopic data for sample 08020 from plagioclase-phyric andesite (L7)

08020 hornblende; 9-Nov-09	**Total fusion age 0.95 ± 0.65 Ma**
Volumes are 1E-13 cm3 NPT	
Neutron flux monitors: 28.030 ± 0.084 Ma FCs (Renne et al., 1998)	
Isotope production ratios: (^{40}Ar/^{39}Ar)K=0.0302±0.00006, (^{37}Ar/^{39}Ar)Ca=1416.4±0.5, (^{36}Ar/^{39}Ar)Ca=0.3952±0.0004,	
Ca/K=1.83 ± 0.01 (37ArCa/39ArK).	J = 0.0048897 ± 0.0000244

Incremental Heating	^{39}Ar(k) (cum %)	Age ± 2 σ (Ma)		^{40}Ar(r) (%)	^{39}Ar(k) (%)	K/Ca ± 2 σ	
2.00 W	0.69	25.29	± 22.45	5.96	0.69	0.367	± 0.149
2.40 W	0.60	22.94	± 61.66	4.44	0.09	0.249	± 0.592
2.90 W	0.87	1.10	± 15.33	0.32	1.48	0.189	± 0.033
3.40 W	2.06	0.77	± 22.34	0.56	1.19	0.081	± 0.013
4.20 W	7.12	0.76	± 2.50	2.20	5.06	0.088	± 0.005
5.20 W	28.20	1.23	± 1.15	11.81	21.08	0.106	± 0.006
6.20 W	68.18	1.04	± 0.63	15.40	39.98	0.082	± 0.004
7.20 W	100.00	1.17	± 1.17	15.45	31.82	0.075	± 0.003

Normal Isochron	^{39}(k)/ ^{36}(a)	± 2 σ	^{40}(a+r)/ ^{36}(a)	± 2 σ	r.i.
2.00 W	6.5	± 0.4	314.2	17.8	0.914
2.40 W	5.3	± 0.7	309.2	38.9	0.965
2.90 W	7.7	± 0.4	296.5	13.4	0.868
3.40 W	19.3	± 3.2	297.2	49.0	0.976
4.20 W	77.7	± 5.7	302.2	22.5	0.965
5.20 W	292.7	± 38.9	336.3	43.3	0.963
6.20 W	480.2	± 56.3	352.0	40.9	0.977
7.20 W	427.2	± 81.0	351.8	67.0	0.985

Inverse Isochron	^{39}(k)/ ^{40}(a+r)	± 2 σ	^{36}(a)/ ^{40}(a+r)	± 2 σ	r.i.
2.00 W	0.021	± 0.001	0.003	0.000180	0.099
2.40 W	0.017	± 0.001	0.003	0.000407	0.010
2.90 W	0.026	± 0.001	0.003	0.000153	0.079
3.40 W	0.065	± 0.002	0.003	0.000555	0.115
4.20 W	0.257	± 0.005	0.003	0.000246	0.167
5.20 W	0.871	± 0.031	0.003	0.000383	0.026
6.20 W	1.364	± 0.034	0.003	0.000330	0.069
7.20 W	1.214	± 0.040	0.003	0.000541	0.110

Isotope Ratios	^{40}(r)/ ^{39}(k)	1 σ	^{40}(r+a)	1 σ	^{40}Ar/ ^{39}Ar	1 σ	^{37}Ar/ ^{39}Ar	1 σ	^{36}Ar/ ^{39}Ar	1 σ
2.00 W	2.880	1.287	0.137	0.00080	48.262	0.583	1.485	0.302	0.154	0.005
2.40 W	2.610	3.531	0.022	0.00007	58.707	0.991	2.193	2.613	0.190	0.012
2.90 W	0.125	0.868	0.233	0.00110	38.380	0.476	2.880	0.248	0.130	0.003
3.40 W	0.087	1.264	0.075	0.00098	15.361	0.276	6.731	0.522	0.053	0.004
4.20 W	0.086	0.142	0.081	0.00063	3.903	0.038	6.164	0.169	0.015	0.000
5.20 W	0.139	0.065	0.100	0.00054	1.175	0.021	5.129	0.152	0.005	0.000
6.20 W	0.118	0.036	0.120	0.00085	0.760	0.009	6.631	0.162	0.004	0.000
7.20 W	0.132	0.066	0.108	0.00141	0.849	0.014	7.286	0.153	0.004	0.000

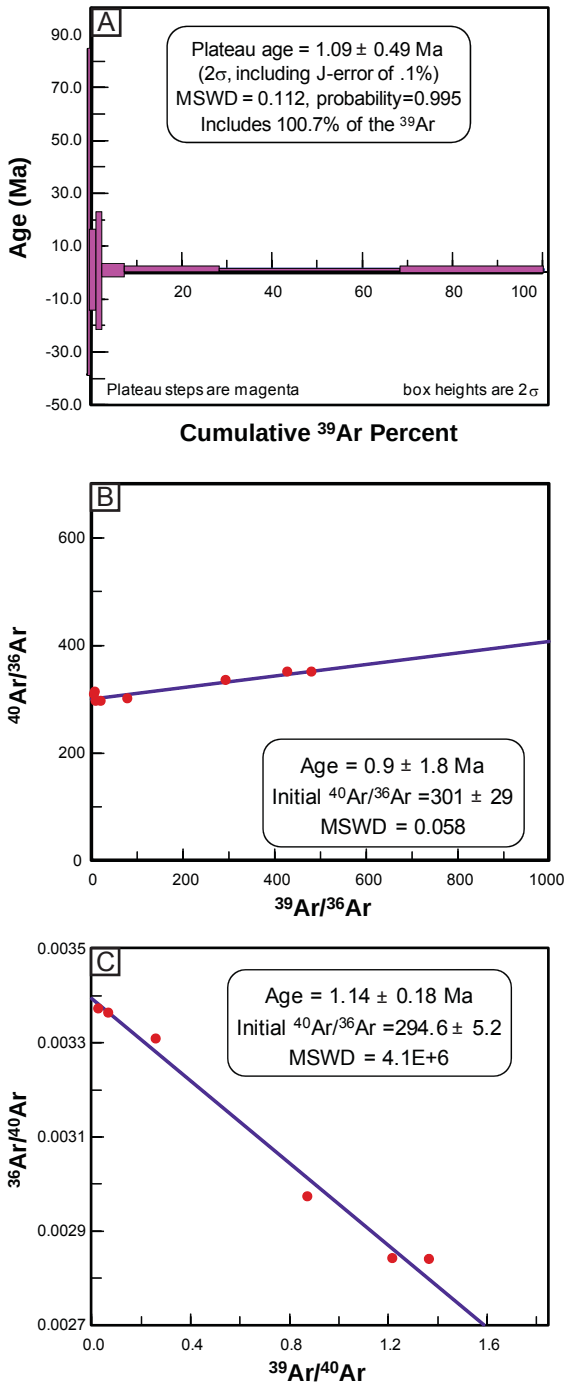

Figure E.1 Preliminary Ar-Ar geochronology results for hornblende from plagioclase-phyric andesite (L8). (A) Plateau age of 1.09 ± 0.49 Ma. (B) Normal isochron age of 0.9 ± 1.8 Ma. (C) Inverse isochron age of 1.14 ± 1.18 Ma.

The samples were analysed on November 9th 2009 at the Noble Gas Laboratory of the Pacific Centre for Isotopic and Geochemical Research (PCIGR) in the Department of Earth and Ocean Sciences at The University of British Columbia. The separates were step-heated at incrementally higher power in the defocused beam of a 10 W CO_2 laser (New Wave

Research MIR10) until fused. The gas evolved from each step was analysed by a VG5400 mass spectrometer equipped with an ion-counting electron multiplier. All measurements were corrected for total system blank, mass spectrometer sensitivity, mass discrimination, radioactive decay during and subsequent to irradiation of Ca, Cl and K (isotope production ratios: (^{40}Ar / ^{39}Ar) K=0.0302, (^{37}Ar / ^{39}Ar) Ca=1416.4306, (^{36}Ar / ^{39}Ar) Ca=0.3952, Ca/K = 1.83, (^{37}ArCa / ^{39}ArK)).

Plateau and correlation ages were calculated using Isoplot v. 3.09 (Ludwig, 2003). Errors are quoted at the 2-sigma (95 % confidence) level and are propagated from all sources except mass spectrometer sensitivity and age of the flux monitor. The best statistically-justified plateau and plateau age were picked based on the following criteria:

1. Three or more contiguous steps comprising more than 50 % of the ^{39}Ar,
2. Probability of fit of the weighted mean age greater than 5 %,
3. Slope of the error-weighted line through the plateau ages equals zero at 5 % confidence
4. Ages of the two outermost steps on a plateau are not significantly different from the weighted-mean plateau age (at 1.8σ six or more steps only),
5. Outermost two steps on either side of a plateau must not have non-zero slopes with the same sign (at 1.8σ nine or more steps only).

E.3 ^{40}Ar / ^{39}Ar results

The Ar-Ar age of the hornblende is reported as 1.09 ± 0.49 Ma but is considered to be imprecise because of the young age and low K concentrations in the hornblende. The sample is currently being reanalysed with the hope of being able to improve the precision. The preliminary age of the plagioclase-phyric andesite is certainly younger than 1.58 Ma.

APPENDIX F

Sample catalogue

Table F.1 Sample catalogue

Field number	UTas catalogue number	Hand sample (HS)	Polished slab (PS)	Thin section (TS)	XRD	XRF	Laser mount (LM)	Map reference		
								Northing	Easting	RL
GW29_223.6	165211	1 HS		1 TS						
GW29_224.9	165212	1 HS			XRD					
GW29_232.25	165213	1 HS			XRD					
GW29_287.25	165214	1 HS								
GW29_287.5	165215	1 HS								
GW29_325.6	165216	1 HS		1 TS	XRD					
GW29_674.10	165217	1 HS								
GW30_376.15	165218	1 HS								
GW30_436.45	165219	1 HS								
GW30_444.9	165220	1 HS		1 TS	XRD					
GW30_501.8	165221	1 HS			XRD					
GW30_538.10	165222	1 HS								
GW30_707.8	165223	1 HS		1 TS						
GW30_751.5	165224	1 HS								
GW30_815.75	165225	1 HS								
GW30_822.2	165226	1 HS		1 TS						
GW31_170.3	165227	1 HS		1 TS	XRD					
GW31_185.5	165228	1 HS			XRD					
GW31_208.4	165229	1 HS		1 TS	XRD					
GW31_238.86	165230	1 HS								
GW31_271.7	165231	1 HS			XRD					
GW31_282.45	165232	1 HS		1 TS	XRD					
GW31_516.6	165233	1 HS								
GW31_697.1	165234	1 HS								
GW32_229.6	165235	1 HS			XRD					
GW32_338.65	165236	1 HS		1 TS	XRD					
GW32_445.7	165237	1 HS								
GW32_772.18	165238	1 HS								
GW32_839.3	165239	1 HS								
GW32_851.3	165240	1 HS								
GW32_882.7	165241	1 HS								
GW32_899.35	165242	1 HS		1 TS						
GW32_919.52	165243	1 HS								
GW33_343.25	165244	1 HS		1 TS						
GW33_384.15	165245	1 HS								

Field number	UTas catalogue number	Hand sample (HS)	Polished slab (PS)	Thin section (TS)	XRD	XRF	Laser mount (LM)	Map reference		
								Northing	Easting	RL
GW33_395.90	165246	1 HS								
GW33_402.5	165247	1 HS		1 TS						
GW33_408.55	165248	1 HS			XRD					
GW33_433.5	165249	1 HS		1 TS						
GW33_723.8	165250	1 HS			XRD					
GW33_763.65	165251	1 HS								
GW33_765.55	165252	1 HS		1 TS						
GW34_325.4	165253	1 HS								
GW34_734.2	165254	1 HS								
IL04_242.5	165255	1 HS		1 TS						
IL04_323.35	165256	1 HS		1 TS						
IL06_64.56	165257	1 HS		1 TS						
DDHL1471_87.6	165258	1 HS			XRD					
DDHL1476_221.5	165259	1 HS			XRD					
DDHL1476_238.37	165260	1 HS			XRD					
DDHL1476_239.1	165261	1 HS		1 TS						
DDHL1476_273.6	165262	1 HS			XRD					
DDHL1476_287.4	165263	1 HS			XRD					
DDHL1456_26.0	165264	1 HS			XRD					
DDHL1456_39.65	165265	1 HS		1 TS	XRD					
DDHL1456_68.4	165266	1 HS								
DDHL1456_78.65	165267	1 HS	PB	1 TS						
DDHL1456_99.5	165268	1 HS								
DDHL1456_137.13	165269	1 HS	PB							
M872_01	165270	1 HS	PB	1 TS				3686	9585	872
M872_02	165271	1 HS		1 TS				3558	9592	872
M872_16Jun06	165272	1 HS		1 TS	XRD			3484	9675	872
M872_18Jul06_1	165273	1 HS			XRD			3724	9657	872
M872_21Jul06_305	165274	1 HS		1 TS	XRD			3640	9552	872
M872_21Jul06_323	165275	1 HS		1 TS	XRD			3656	9549	872
M872_26Jul06_ CHIM	165276	1 HS						3668	9561	872
M884_04Jul06_130	165277	1 HS		1 TS	XRD			3924	9695	884
M884_11Jul06_150	165278	1 HS		1 TS	XRD			3680	9904	884
M884_11Jul06_44.4	165279	1 HS		1 TS	XRD			3800	9900	884
M884_13Jul06_98	165280	1 HS	PB					3502	9850	884
M884_29Jun06	165281	1 HS	PB	1 TS				3840	9910	884
M884_30Jun06_10	165282	1 HS		1 TS				3756	9514	884
M972_16Jun06	165283	1 HS						3976	10038	972
DDHL1408_73.58	165284	1 HS								
DDHL1408_90.61	165285	1 HS	PB							
DDHL1415_36.04	165286	1 HS								
DDHL1415_78.18	165287	1 HS	PB							
DDHL1415_110.13	165288	1 HS		1 TS						

Field number	UTas catalogue number	Hand sample (HS)	Polished slab (PS)	Thin section (TS)	XRD	XRF	Laser mount (LM)	Map reference		
								Northing	Easting	RL
DDHL1415_118.52	165289	1 HS	PB							
DDHL1415_122.17	165290	1 HS	PB							
DDHL1415_134.32	165291	1 HS	PB							
DDHL1415_134.86	165292	1 HS		1 TS						
DDHL1415_154.3	165293	1 HS								
DDHL1415_166.12	165294	1 HS	PB	1 TS		XRF				
DDHL1446_10.36	165295	1 HS	PB	1 TS						
DDHL1446_33.55	165296	1 HS	PB							
DDHL1446_37.7	165297	1 HS	PB							
DDHL1446_44.35	165298	1 HS		1 TS						
DDHL1446_60.2	165299	1 HS		1 TS						
DDHL1446_60.33	165300	1 HS	PB							
DDHL1446_64.1	165301	1 HS	PB	1 TS						
DDHL1446_70.43	165302	1 HS	PB							
DDHL1446_77.4	165303	1 HS	PB							
DDHL1446_131.40	165304	1 HS								
DDHL1446_154.12	165305	1 HS	PB	1 TS						
DDHL1446_169.6	165306	1 HS	PB							
DDHL1448_4.1	165307	1 HS								
DDHL1448_50	165308	1 HS	PB							
DDHL1448_51.84	165309	1 HS	PB							
DDHL1448_52.53	165310	1 HS	PB	1 TS						
DDHL1448_53	165311	1 HS		1 TS						
DDHL1448_56.23	165312	1 HS	PB							
DDHL1448_59.6	165313	1 HS								
DDHL1448_61.8	165314	1 HS		1 TS						
DDHL1448_67.37	165315	1 HS	PB							
DDHL1448_68.6	165316	1 HS	PB							
DDHL1448_85.1	165317	1 HS	PB							
DDHL1448_88.58	165318	1 HS								
DDHL1448_90.08	165319	1 HS		1 TS						
DDHL1448_118.47	165320	1 HS	PB	1 TS						
DDHL1448_149.5	165321	1 HS	PB							
DDHL1449_49.83	165322	1 HS								
DDHL1449_58.53	165323	1 HS	PB							
DDHL1449_61.6	165324	1 HS	PB							
DDHL1449_78.75	165325	1 HS		1 TS						
DDHL1449_93.22	165326	1 HS								
DDHL1449_93.75	165327	1 HS								
DDHL1449_95.2	165328	1 HS	PB							
DDHL1449_95.83	165329	1 HS	PB							
DDHL1449_99.58	165330	1 HS								
DDHL1449_101	165331	1 HS		1 TS						

Field number	UTas catalogue number	Hand sample (HS)	Polished slab (PS)	Thin section (TS)	XRD	XRF	Laser mount (LM)	Map reference		
								Northing	Easting	RL
DDHL1449_103.57	165332	1 HS								
DDHL1449_114.72	165333	1 HS		1 TS						
DDHL1449_119.8	165334	1 HS								
DDHL1449_137.52	165335	1 HS		1 TS						
DDHL1450_50.7	165336	1 HS		1 TS						
DDHL1450_70.74	165337	1 HS		1 TS						
DDHL1450_71.66	165338	1 HS		1 TS						
DDHL1450_77.1	165339	1 HS	PB							
DDHL1450_80.5	165340	1 HS		1 TS						
DDHL1450_84.95	165341	1 HS								
DDHL1450_95.97	165342	1 HS								
DDHL1450_114.27	165343	1 HS		1 TS						
DDHL1450_114.8	165344	1 HS	PB							
DDHL1450_115	165345	1 HS	PB							
DDHL1455_5.9	165346	1 HS	PB							
DDHL1455_24.18	165347	1 HS	PB							
DDHL1455_41.0	165348	1 HS								
DDHL1455_65.07	165349	1 HS	PB							
DDHL1455_71.9	165350	1 HS								
DDHL1455_74.67	165351	1 HS	PB							
DDHL1455_85.48	165352	1 HS	PB							
DDHL1455_86.1	165353	1 HS								
DDHL1455_105.05	165354	1 HS		1 TS						
DDHL1455_131.58	165355	1 HS								
DDHL1502_165.4	165356	1 HS	PB							
DDHL1502_283.42	165357	1 HS	PB							
DDHL1502_323.8	165358	1 HS	PB							
DDHL712_214.04	165359	1 HS		1 TS						
DDHL757_211.25	165360	1 HS		1 TS						
DDHL757_212.86	165361	1 HS		1 TS						
DDHL757_224.7	165362	1 HS	PB	1 TS						
DDHL757_246.13	165363	1 HS	PB	1 TS						
DDHL757_252.21	165364	1 HS	PB							
DDHL757_252.72	165365	1 HS		1 TS						
DDHL757_254.07	165366	1 HS	PB							
DDHL757_260.4	165367	1 HS	PB							
DDHL757_260.73	165368	1 HS		1 TS						
DDHL757_285.06	165369	1 HS	PB							
DDHL757_319.33	165370	1 HS		1 TS						
DDHL757_324.55	165371	1 HS	PB							
DDHL757_327.8	165372	1 HS	PB	1 TS						
DDHL791_152.1	165373	1 HS		1 TS						
DDHL791_170.86	165374	1 HS	PB							

Field number	UTas catalogue number	Hand sample (HS)	Polished slab (PS)	Thin section (TS)	XRD	XRF	Laser mount (LM)	Map reference		
								Northing	Easting	RL
DDHL791_186.73	165375	1 HS								
DDHL791_192.34	165376	1 HS		1 TS						
DDHL791_200.83	165377	1 HS		1 TS						
DDHL791_227.7	165378	1 HS								
DDHL791_228.6	165379	1 HS		1 TS						
DDHL791_231.15	165380	1 HS		1 TS						
DDHL791_233.4	165381	1 HS								
DDHL791_238.05	165382	1 HS	PB	1 TS						
DDHL791_240.53	165383	1 HS	PB							
DDHL791_242.26	165384	1 HS		1 TS						
DDHL791_293.48	165385	1 HS	PB							
DDHL791_304.45	165386	1 HS	PB	1 TS						
DDHL1285_51.67	165387	1 HS		1 TS						
DDHL1285_54.83	165388	1 HS								
DDHL1160_145.48	165389	1 HS		1 TS						
DDHL1160_169.34	165390	1 HS	PB							
DDHL1160_170.2	165391	1 HS		1 TS						
DDHL1160_173.05	165392	1 HS		2 TS						
DDHL1160_180.96	165393	1 HS	PB							
DDHL1160_202.13	165394	1 HS	PB	1 TS						
DDHL1160_212.35	165395	1 HS								
DDHL1160_230.95	165396	1 HS	PB	1 TS						
DDHL1160_299.1	165397	1 HS		1 TS						
DDHL1160_313.45	165398	1 HS	PB							
DDHL1703_31.60	165399	1 HS								
DDHl1703_32.95	165400	1 HS	PB	1 TS						
DDHl1703_43.75	165401	1 HS	PB	1 TS						
DDHl1703_50.35	165402	1 HS	PB	1 TS						
DDHl1703_55	165403	1 HS		1 TS						
DDHL1703_62.50	165404	1 HS								
DDHl1703_87.4	165405	1 HS	PB	1 TS						
DDHl1703_99.1	165406	1 HS	PB	1 TS						
DDHl1703_113.2	165407	1 HS	PB	1 TS						
DDHl1703_137.08	165408	1 HS		1 TS						
DDHL1704_87.58	165409	1 HS	PB	1 TS						
DDHL1704_95.65	165410	1 HS	PB	1 TS						
DDHL1704_109.5	165411	1 HS	PB	1 TS						
DDHL1704_123	165412	1 HS		1 TS						
DDHL1704_134.55	165413	1 HS	PB	1 TS						
DDHL1708_45.0	165414	1 HS								
DDHL1708_92.9	165415	1 HS	PB	1 TS						
L968_29Jul06a	165416	1 HS	PB	1 TS				4293	8876	968
L9868_29Jul06b	165417	1 HS		1 TS				4120	8854	968

Field number	UTas catalogue number	Hand sample (HS)	Polished slab (PS)	Thin section (TS)	XRD	XRF	Laser mount (LM)	Map reference		
								Northing	Easting	RL
L968_07003	165418	1 HS						4253	8890	968
L854_07007	165419	1 HS	PB	1 TS				4158	8996	854
LPH6 ramp_07008	165420	1 HS						4169	8882	956
L854_07010	165421	1 HS	PB					4186	9217	854
L854_07011	165422	1 HS						4186	9217	854
L968_07015	165423	1 HS	PB	1 TS				4342	8962	968
L968_07016	165424	1 HS	PB					4321	8944	968
L968_07018	165425	1 HS	PB					4191	8871	968
L980_07021	165426	1 HS	PB					4262	8868	980
L920_08002	165427	1 HS						4448	9226	920
L920_08004	165428	1 HS						4448	9235	920
L920_08007	165429	1 HS	PB	1 TS				3899	9767	920
L920_08008	165430	1 HS	PB					3899	9767	920
L920_08009	165431	1 HS	PB					3899	9767	920
L920_08011	165432	1 HS		1 TS				3912	9782	920
L920_08015	165433	1 HS	PB					4176	9885	920
LPh7upper_08017a	165434	1 HS						4436	8518	977
LPh7upper_08017b	165435	1 HS						4436	8515	977
08020_L992	165436	1 HS		1 TS		XRF		4156	8791	992
08021_M908	165437	1 HS				XRF		3241	9661	908
08022_L920	165438	1 HS		1 TS		XRF		3885	9755	920
08023_LPH6 ramp	165439	1 HS		1 TS		XRF		4007	9178	868
08024_LPH6 ramp	165440	1 HS		1 TS		XRF		4101	9109	867
08025_Quarry	165441	1 HS		1 TS		XRF		9008	7889	-
Lmst_1	165442	1 HS		1 TS			LM	5030	11852	1000
Lmst_2	165443	1 HS		1 TS			LM	5030	11854	1001
Lmst_3	165444	1 HS		1 TS			LM	5045	11831	1003
Lmst_4	165445	1 HS		1 TS			LM	5035	11828	1012
Lmst_5	165446	1 HS		1 TS			LM	5037	11820	1014
Lmst_6	165447	1 HS		1 TS			LM	5029	11832	1015
Lmst_7	165448	1 HS		1 TS			LM	5030	11844	1040
Lmst_12.1	165449	1 HS		1 TS			LM	4896	11530	1012
Lmst_9.3	165450	1 HS		1 TS			LM	5080	11500	-